

Calibration of distorted wave Born approximation for electron impact excitation of Ne and Ar at incident energies below 100 eV

Yaqiu Liang¹, Zhangjin Chen², D. H. Madison³ and C. D. Lin²

¹ College of Physics, Liaoning University, Shenyang 110036, People's Republic of China

² J. R. Macdonald Laboratory, Physics Department, Kansas State University, Manhattan, Kansas 66506-2604, USA

³ Physics Department, Missouri University of Science and Technology, Rolla, Missouri 65401, USA

Abstract.

We calibrate the distorted wave Born approximation (DWBA) for electron impact excitation processes empirically. Differential cross sections (DCS) for the excitation of the $2p^53s$, $2p^53p$, $2p^54s$, and $2p^54p$ configurations of Ne and the $3p^54s$ and $3p^54p$ configurations of Ar by electron impact are calculated using DWBA for incident energies between 20 and 100 eV. The calculated results are compared with the absolute experimental measurements and other theoretical results. We found that the structure of the DCS can be well reproduced by the DWBA model while the magnitude is overestimated for most cases considered here. The differences in magnitude between DWBA and experiment are used to test the calibration of DWBA such that the DWBA can be used to describe laser-induced electron impact excitation processes. These processes are involved in the non-sequential double ionization of atoms in strong laser fields.

PACS numbers: 34.80.Dp, 34.50.Rk

Submitted to: *J. Phys. B: At. Mol. Opt. Phys.*

1. Introduction

The process of electron impact excitation of atoms and ions is one of the most basic and important processes in atomic physics. Numerous theoretical methods have been used for the process calculations, including distorted wave Born approximation (DWBA) [1], second-order distorted wave model [2], R -matrix method [3], and convergent close-coupling (CCC) calculations [4], among which the DWBA is the simplest. The sophisticated theoretical models, such as CCC and R -matrix method, are capable of reproducing accurate angular differential cross sections (DCS), as well as the absolute magnitude. They are more suitable for low incident energies. For higher energies, both the integrated and differential cross sections predicted by DWBA are fairly accurate. However, it has been well recognized that, at low energies, the total cross sections (TCS) predicted by the DWBA significantly exceed the experimental values. Ideally, one would use the R -matrix approach for low energies, the DWBA for high energies, but at intermediate energies, neither method is efficient if a large amount of data is needed.

The purpose of this work is to correct (by renormalization) the DWBA predictions empirically such that the DCS calculated from DWBA can be used for low collision energies. We will use the empirical formula proposed by Tong *et al.* [5] for the total excitation cross sections. Our ultimate objective is to apply the calibrated DWBA (C-DWBA) to simulate the correlated momentum distributions in nonsequential double ionization (NSDI) of atoms in strong laser fields.

The process of NSDI of atoms in linearly polarized laser pulses is one of the most interesting and challenging topics in strong field physics. In NSDI, one electron that is first released near the maximum of the oscillating electric field may be driven back to revisit the parent ion when the electric field is near zero. When the returning electron collides with the parent ion with energies above the ionization threshold, it may kick out another bound electron, resulting in an (e, 2e)-like process. The returning electron may also excite the bound electron to a higher excited state which is subsequently tunnel ionized when the electric field increases again. Since the year of 2000, complete experimental measurements on the full momentum vectors of the two outgoing electrons along the direction of polarization of the laser pulse have become available [6, 7], and a number of theoretical studies have also been carried out.

Recently, Chen *et al.* [8] have developed a quantitative rescattering (QRS) theory which has been applied to various rescattering processes induced by short intense laser pulses [9, 10, 11, 12, 13, 14]. The significant advantage of the QRS theory is that it treats the rescattering processes in the laser field as laser-*free* scattering processes, where the laser-induced returning electrons are described by a wavepacket. The QRS enables us to simulate two-dimensional correlated momentum distributions for NSDI *quantitatively* by calculating the triple differential cross sections (TDCS) for (e, 2e) [13] and the DCS for electron impact excitation of ions [14]. However, to obtain the correlated momentum spectra that can be compared with experimental measurements, one needs to evaluate the TDCS for (e, 2e) and the DCS for excitation for all possible momenta of the returning

electrons. For NSDI of atoms in strong laser pulses, the highest energy, E_i^{\max} , of the returning (incident) electron is determined by the laser field, which is less than 100 eV for typical 800 nm lasers. To simulate the correlated momentum distributions for NSDI, the DCS's for electron impact excitation of the parent ion at all incident energies from threshold to E_i^{\max} are needed. To reduce the computational effort a simple and efficient theoretical model is desirable. In this work, we develop the C-DWBA for this purpose.

The organization of this paper is as follows: In section II, the basic theory of DWBA for electron impact excitation is presented and the method to calibrate DWBA is introduced. In section III, the DCS of DWBA for electron impact excitation of Ne and Ar at incident energies below 100 eV are normalized and compared with the absolute experimental data. The normalization factors are then used to test the calibration for DWBA.

Atomic units are used in this paper unless otherwise specified.

2. Theory

In this section, we present the DWBA theory on electron impact excitation of atoms and the method to calibrate the DWBA at low energies. The formulas presented here are generic and therefore can be easily applied to the processes of electron impact excitation of ions which are involved in NSDI.

2.1. DWBA

Suppose we have an electron with momentum \mathbf{k}_i which collides with an atom A , after the collision, the scattered electron has momentum \mathbf{k}_f , and one bound electron in atom A is excited to a higher energy bound state. In the frozen core approximation, the “exact” Hamiltonian for the whole system is

$$H = -\frac{1}{2}\nabla_1^2 + V_{A^+}(r_1) - \frac{1}{2}\nabla_2^2 + V_{A^+}(r_2) + \frac{1}{r_{12}}. \quad (1)$$

where \mathbf{r}_1 and \mathbf{r}_2 are the position vectors for the projectile and the bound state electron with respect to the nucleus, respectively. This Hamiltonian can be rewritten approximately as

$$H_j = -\frac{1}{2}\nabla_1^2 + U_j(r_1) - \frac{1}{2}\nabla_2^2 + V_{A^+}(r_2) \quad (j = i, f). \quad (2)$$

In this equation, U_i (U_f) is the distorting potential used to calculate the initial (final) state wave function $\chi_{\mathbf{k}_i}$ ($\chi_{\mathbf{k}_f}$) for the projectile. In the distorted wave Born approximation, the direct transition amplitude for excitation from an initial state Ψ_i to a final state Ψ_f is expressed by

$$f = \langle \chi_{\mathbf{k}_f}^-(1)\Psi_f(2) | V_i | \Psi_i(2)\chi_{\mathbf{k}_i}^+(1) \rangle, \quad (3)$$

where V_i is the perturbation interaction,

$$V_i = H - H_i = \frac{1}{r_{12}} + V_{A^+}(r_1) - U_i(r_1). \quad (4)$$

In Eq. (3), the initial and final state wave functions for the projectile satisfy the differential equation

$$\left[-\frac{1}{2}\nabla_1^2 + U_j(r_1) - \frac{1}{2}k_j^2\right]\chi_{\mathbf{k}_j}(\mathbf{r}_1) = 0 \quad (j = i, f), \quad (5)$$

and the bound state wave functions are eigenfunctions of the equation

$$\left[-\frac{1}{2}\nabla_2^2 + V_{A^+}(r_2) - \epsilon_j\right]\Psi_j(\mathbf{r}_2) = 0 \quad (j = i, f), \quad (6)$$

where ϵ_j ($j = i, f$) are the corresponding eigenenergies of the initial and final bound states which can be expressed as

$$\Psi_j(\mathbf{r}) = \psi_{N_j L_j}(r) Y_{L_j M_j}(\hat{\mathbf{r}}) \quad (j = i, f). \quad (7)$$

The exchange scattering amplitude is given by

$$g = \langle \Psi_f(1) \chi_{\mathbf{k}_f}^-(2) | V_i | \Psi_i(2) \chi_{\mathbf{k}_i}^+(1) \rangle. \quad (8)$$

Finally, the differential cross section for electron impact excitation is given by

$$\begin{aligned} \frac{d\sigma}{d\Omega} &= N(2\pi)^4 \frac{k_f}{k_i} \frac{1}{2L_i + 1} \\ &\times \sum_{M_i=-L_i}^{+L_i} \sum_{M_f=-L_f}^{+L_f} \left(\frac{3}{4} |f - g|^2 + \frac{1}{4} |f + g|^2 \right). \end{aligned} \quad (9)$$

The prefactor N in Eq. (9) denotes the number of electrons in the subshell from which one electron is excited.

The distorting potentials, U_i and U_f , used in Eq. (5) to calculate the wave functions for the projectile in the initial and final states, respectively, are not determined directly by the formalism. Here, we use static potentials which take the form as

$$U_j(r_1) = V_{A^+}(r_1) + \int d\mathbf{r}_2 \frac{|\Psi_j(\mathbf{r}_2)|^2}{r_{12}} \quad (j = i, f). \quad (10)$$

As shown previously, $V_{A^+}(r)$ in Eq. (10) is the atomic potential used to evaluate eigenstate wave functions of the bound state electron. Here we use the effective potential from Tong and Lin [15] based on single active electron approximation, which is given by

$$V_{A^+}(r) = -\frac{1 + a_1 e^{-a_2 r} + a_3 r e^{-a_4 r} + a_5 e^{-a_6 r}}{r}, \quad (11)$$

where the parameters a_i , as given explicitly in table 1 in Tong and Lin [15], are obtained by fitting the calculated binding energies from this potential to the experimental ones of the ground state and the first few excited states of the target atom.

2.2. Calibration of DWBA

The overestimate of DWBA on DCS can be corrected by using the empirical method proposed by Tong *et al.* [5] to evaluate the total cross sections for electron impact excitation:

$$\sigma_{\text{Tong}}(E_i) = \alpha \frac{\pi}{\Delta E^2} e^{1.5(\Delta E - \epsilon)/E_i} f\left(\frac{E_i}{\Delta E}\right), \quad (12)$$

where

$$f(x) = \frac{1}{x} \left[\beta \ln x - \gamma \left(1 - \frac{1}{x} \right) + \delta \frac{\ln x}{x} \right]. \quad (13)$$

In Eq. (12), ΔE is the excitation energy for a given transition, ϵ is the eigenenergy of the corresponding excited state. The original formula given by Tong *et al.* does not have the prefactor α which is added in the present work to ensure that it reproduces the same cross sections as those from DWBA at high energies. The parameters in Eq. (13) have been obtained initially by fitting to the convergent-close coupling excitation cross sections for hydrogen and He^+ . Explicitly, these parameters are $\beta = 0.7638$, $\gamma = 1.1759$, and $\delta = 0.6706$.

The total cross section of DWBA at fixed incident energy $E_i = k_i^2/2$ can be obtained from Eq. (9) by

$$\sigma_{\text{DWBA}}(E_i) = \int \frac{d\sigma}{d\Omega} d\hat{\mathbf{k}}_f. \quad (14)$$

By matching the total cross sections from Eq. (12) with those from Eq. (14) at high incident energies, say $E_i = 500$ eV, one obtains the prefactor α in Eq. (12) for excitation of each configuration. To calibrate the DWBA at low energies, we define a scaling factor

$$\mathcal{C}(E_i) = \sigma_{\text{Tong}}(E_i)/\sigma_{\text{DWBA}}(E_i). \quad (15)$$

It is the the scaling factor in Eq. (15) that should be used to normalize the differential cross sections of DWBA at different incident energies.

3. Results and discussions

The perturbative nature of DWBA makes it overestimate electron impact excitation cross sections of ions at low energies. To calibrate the DWBA theory, one should compare its predictions to accurate theoretical results or absolute experimental measurements. Unfortunately, neither are easily available for atomic and molecular ions. Thus we use neutral Ne and Ar atoms for the calibration.

In Figures 1-4, the DCS's for the excitation of the $2p^53s$, $2p^53p$, $2p^54s$ and $2p^54p$ configurations of Ne for incident energies below 100 eV from DWBA are compared with the absolute experimental data [16, 17]. For the $2p^53s$ configuration, the DCS's from the *R*-matrix theory are also plotted for incident energies of 30 and 25 eV. It can be seen from Figs. 1-4 that the DWBA overestimates the DCS's for all the cases considered here. To get best overall agreement, different normalization factors are assigned to the DWBA for different configurations and different incident energies. For incident energies below 30 eV, the DCS's of DWBA could be 2-7 times higher than the experimental measurements. To see the distorting effect from the DWBA, the results of plane wave Born approximation (PWBA), in which plane waves are used to describe the projectile electron in both the initial and final states, are also displayed for comparison. For scattering angles greater than 30° , one can see that the PWBA fails completely in predicting the angular distributions even for incident energy of 100 eV. In contrast, the

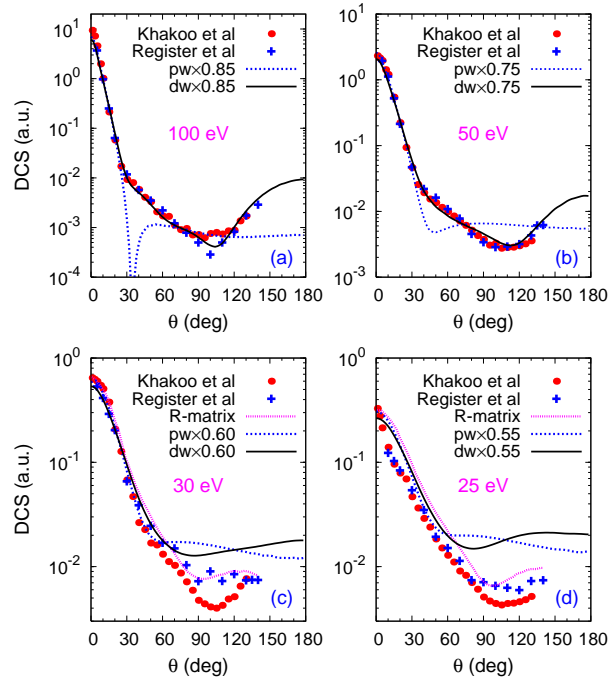


Figure 1. DCS for the excitation of the $2p^5 3s$ configuration of Ne by electron impact at incident energies of (a) 100 eV, (b) 50 eV, (c) 30 eV, and (d) 25 eV. The absolute experimental measurements are from Register *et al.* [16] and Khakoo *et al.* [17]. For incident energies of 30 and 25 eV, the results of *R*-Matrix from Khakoo *et al.* [17] are also plotted for comparison.

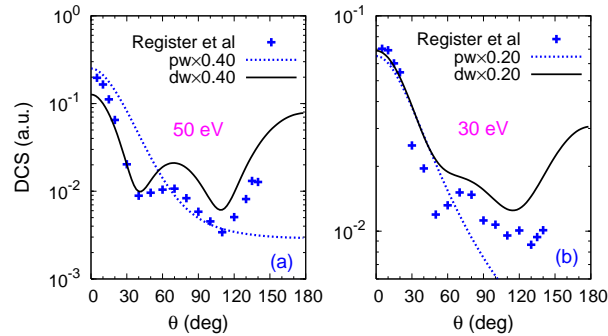


Figure 2. Same as Fig. 1 but for configuration of $2p^5 3p$ at incident energies of (a) 50 eV and (b) 30 eV.

enhanced DCS's for backward scattering observed in experiment are well reproduced by the DWBA.

In Figs. 5 and 6, we show similar comparison for the excitation of $3p^5 4s$ and $3p^5 4p$ configurations of Ar. The experimental measurements were performed by Chutjian and Cartwright [18]. Compared to the excitation of Ne, the DCS of Ar have more structures. For example, for $3p^5 4s$ at 100 eV and 50 eV, as shown in Figs. 5(a,b), in addition to the rapid slope change around 25° , extra minima were observed in experiment which are reproduced by the DWBA. For $3p^5 4p$ at 100 eV and 50 eV, as shown in Figs. 6(a,b),

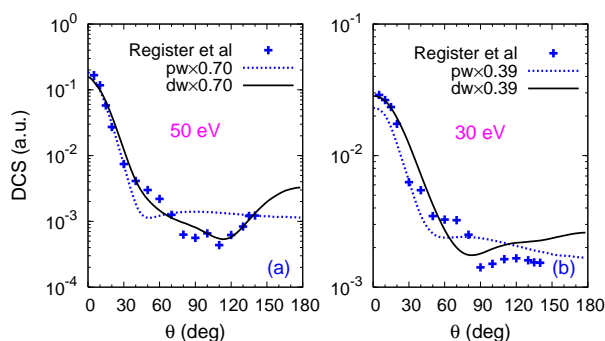


Figure 3. Same as Fig. 1 but for the $2p^5 4s$ configuration at incident energies of (a) 50 eV and (b) 30 eV.

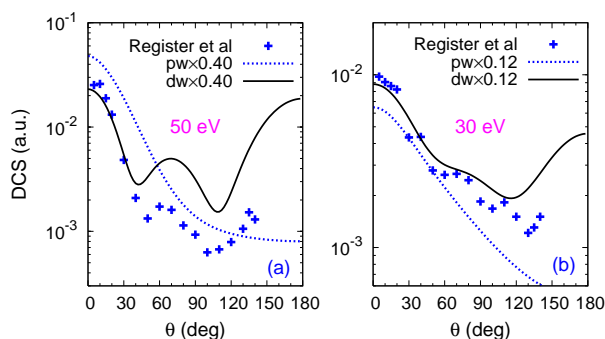


Figure 4. Same as Fig. 1 but for the $2p^5 4p$ configuration at incident energies of (a) 50 eV and (b) 30 eV.

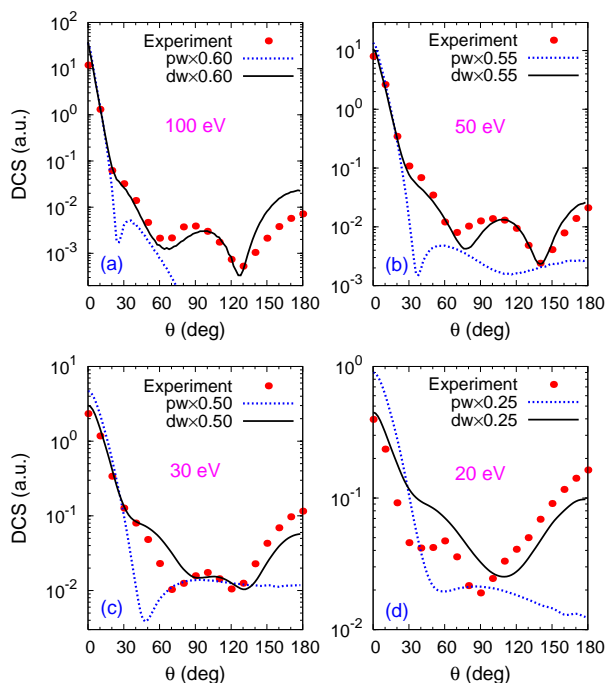


Figure 5. DCS for the excitation of the $3p^5 4s$ configuration of Ar by electron impact at incident energies of (a) 100 eV, (b) 50 eV, (c) 30 eV and (d) 20 eV. The absolute experimental measurements are from Chutjian and Cartwright [18].

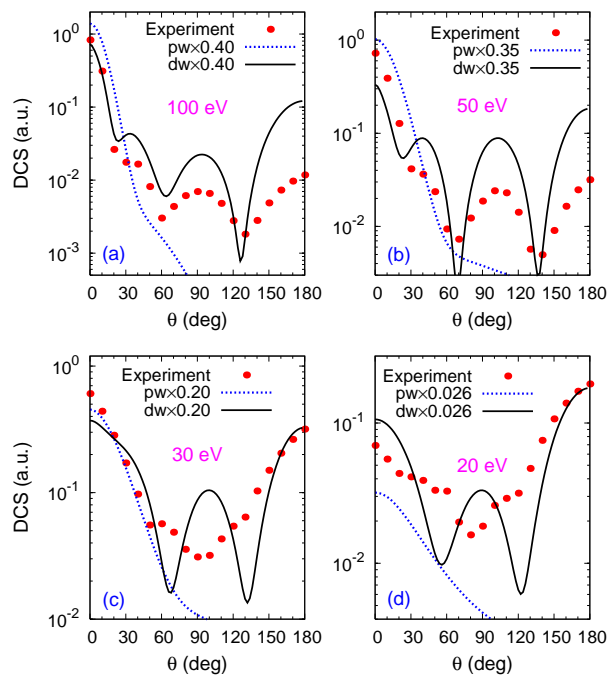


Figure 6. Same as Fig. 5 but for the $3p^5 4p$ configuration at incident energies of (a) 100 eV, (b) 50 eV, (c) 30 eV, and (d) 20 eV.

DWBA predicts triple minima in the DCS. They were observed in experiment as well despite that the backscattering is overestimated by the DWBA. This might indicate that the distorting potential used in the calculations needs to be improved. For lower incident energies of 30 eV and 20 eV, the agreement between DWBA and experiment for $3p^5 4p$ of Ar can not be regarded as satisfactory. However, the main feature can still be predicted by the DWBA. It should be noted that, for the excitation of $3p^5 4p$ of Ar at 20 eV (see Fig. 6(d)), the yield from DWBA exceeds the experimental value by an even greater margin than the PWBA result. For this case, the DWBA predicts the DCS which is about 40 times higher than experiment.

The empirical formula, Eq. (12), has already been used to calculate the total ionization yield of Ar in NSDI as a function of the peak intensity for a linearly polarized laser pulse by Micheau *et al.* [12].

To obtain the scaling factor $\mathcal{C}(E_i)$ for electron-Ne excitation, we calculate the TCS's using DWBA and those using Eq. (12) for all the four configurations considered here at incident energies from threshold up to 500 eV. These TCS's for incident energies below 120 eV are plotted in Fig. 7 referring to the left vertical axis. It can be seen that the difference in the magnitude of TCS between DWBA and Tong *et al* increases with decreasing incident energy. This difference is indicated by the the scaling factor $\mathcal{C}(E_i)$ which is also plotted in Fig. 7, referring to the right vertical axis. To see the accuracy of the scaling factor, the normalization factors used in Figs. 1-4 for DWBA to obtain the best overall agreement with the experimental DCS's are displayed for comparison. One can see that all the normalization factors used in Figs. 1-4 agree well

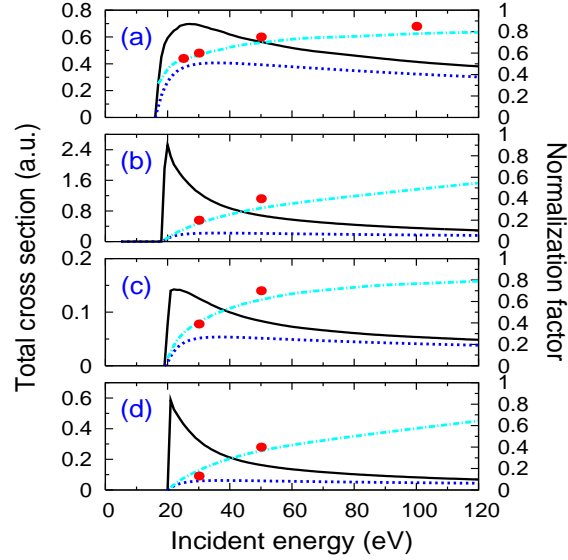


Figure 7. Total cross sections (left vertical axis) and normalization factors of DWBA (right vertical axis) for electron impact excitation of Ne from $2p^6$ to (a) $2p^5 3s$, (b) $2p^5 3p$, (c) $2p^5 4s$, and (d) $2p^5 4p$. Solid curve, total cross sections of DWBA; Dotted curve, total cross sections calculated using the empirical formula of Tong *et al.* [5]; Chain curve, scaling factor $\mathcal{C}(E_i)$; Solid circles, normalization factors used in Figs. 1-4 for DWBA to obtain the best overall agreement with experiment.

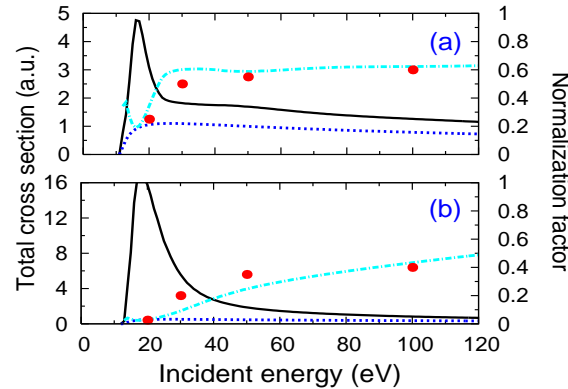


Figure 8. Same as Fig. 7 but for Ar from $3p^6$ to (a) $3p^5 4s$ and (b) $3p^5 4p$. The solid circles are the normalization factors used in Figs. 5 and 6 for DWBA to obtain the best overall agreement with experiment.

with those predicted by the scaling factor $\mathcal{C}(E_i)$. In Fig. 8, similar comparisons for Ar are shown. The good agreement of $\mathcal{C}(E_i)$ with the normalization factors used in Figs. 5 and 6 confirms again the validity of the calibration method.

In conclusion, we proposed a method to calibrate the DCS from DWBA for electron impact excitation of atoms at low energies. The method will be applied to simulate the correlated electron momentum spectra for NSDI of atoms in a strong laser field, in which electron impact excitation of the ions is involved. This work paves the way for theoretical study, based on the QRS model, on NSDI of atoms in strong laser pulse.

Acknowledgment

This work was supported in part by Chemical Sciences, Geosciences and Biosciences Division, Office of Basic Energy Sciences, Office of Science, US Department of Energy. Y Liang was supported with financial aids from China Scholarship Council, China Education Ministry under Grant No. 2009-1590, and Education Department in Liaoning Province of China under Grant No. 2009A305. The work of D.H.M. was supported by the National Science Foundation under Grant No. PHY-0757749.

References

- [1] Bartschat K and Madison D H 1987 *J. Phys. B: At. Mol. Opt. Phys.* **20** 5839
- [2] Madison D H and Winters K H 1983 *J. Phys. B: At. Mol. Opt. Phys.* **16** 4437
- [3] Zeman V and Bartschat K 1997 *J. Phys. B: At. Mol. Opt. Phys.* **30** 4609
- [4] Bray Igor and Stelbovics Andris T 1992 *Phys. Rev. A* **46** 6995
- [5] Tong X M, Zhao Z. X and Lin C D 2003 *Phys. Rev. A* **68** 043412
- [6] Weber Th, Giessen H, Weckenbrock M, Urbasch G, Staudte A, Spielberger L, Jagutzki O, Mergel V, Vollmer M and Dörner R 2000 *Nature (London)* **405** 658
- [7] Staudte A, Ruiz C, Schöffler M, Schössler S, Zeidler D, Weber Th, Meckel M, Villeneuve D M, Corkum P B, Becker A and Dörner R 2007 *Phys. Rev. Lett.* **99** 263002
- [8] Chen Zhangjin, Le Anh-Thu, Morishita Toru and Lin C D 2009 *Phys. Rev. A* **79** 033409
- [9] Lin C D, Le Anh-Thu, Chen Zhangjin, Morishita Toru and Lucchese Robert 2009 *J. Phys. B: At. Mol. Opt. Phys.* **43** 122001
- [10] Chen Zhangjin, Wittmann T, Horvath B and Lin C D 2009 *Phys. Rev. A* **80** 061402(R)
- [11] Yaqiu Liang 2010 *Phys. Rev. A* **82** 055403
- [12] Micheau Samuel, Chen Zhangjin, Le Anh-Thu and Lin C D 2009 *Phys. Rev. A* **79** 013417
- [13] Chen Zhangjin, Liang Yaqiu and Lin C D 2010 *Phys. Rev. Lett.* **104** 253201
- [14] Chen Zhangjin, Liang Yaqiu and Lin C D 2010 *Phys. Rev. A* **82** 063417
- [15] Tong X M and Lin C D 2005 *J. Phys. B: At. Mol. Opt. Phys.* **38** 2593
- [16] Register D F, Trajmar S, Steffensen G and Cartwright David C 1984 *Phys. Rev. A* **29** 1793
- [17] Khakoo M A, Wrkich J, Larsen M, Kleiban G, Kanik I, Trajmar S, Brunger M J, Teubner P J O, Crowe A, Fontes C J, Clark R E H, Zeman V, Bartschat K, Madison D H, Srivastava R and Stauffer A D 2002 *Phys. Rev. A* **65** 062711
- [18] Chutjian A and Cartwright D C 1981 *Phys. Rev. A* **23** 2178